



OPEN

Mechanical and esthetic properties of denture base resins in relation to thermocycling

Ha Eun Choi¹, Sumin Kim², Gi Youn Kim², Jiayi Li³, Stefano Pieralli⁴ & Kyung Chul Oh²✉

This study evaluated the shear bond strength (SBS), flexural strength, and color stability of three denture base resins (DBRs)—heat-polymerized (HEA), cold-polymerized (COL), and 3D-printed (TDP)—before and after thermocycling. SBS was evaluated after bonding COL to each DBR. Flexural strength was measured via three-point bending, and color stability with a colorimeter. Half of the specimens underwent 10,000 thermocycles to simulate aging. TDP (9.91 MPa) showed significantly lower SBS than HEA (14.85 MPa) and COL (15.76 MPa) before thermocycling ($p < 0.001$), but was comparable to HEA (6.89 vs. 7.17 MPa; $p > 0.999$) afterward. SBS decreased significantly in all groups post-thermocycling ($p < 0.01$). Thermocycling did not affect the flexural strength of HEA ($p = 0.841$) or COL ($p = 0.434$), but significantly reduced TDP's flexural strength (87.55 to 79.79 MPa; $p = 0.002$), which nevertheless remained significantly higher than those of HEA and COL ($p < 0.001$). TDP exhibited the highest color change ($\Delta E_{00} = 3.23$), significantly greater than HEA (0.83; $p < 0.001$) and COL (1.94; $p = 0.002$), exceeding the perceptibility threshold. While 3D-printed DBRs exhibited comparable SBS and flexural strength to heat-polymerized DBRs after thermocycling, their esthetic durability remains limited under simulated aging.

Keywords Color stability, Denture base resin, Flexural strength, Shear bond strength, Thermocycling, 3D printing

Acrylic resin has been widely used in dentistry for decades and has continuously improved in terms of physical properties and biocompatibility. Among various dental materials, polymethyl methacrylate (PMMA) remains the most commonly used denture base resin (DBR) due to its ease of fabrication, adequate strength, low toxicity, and esthetic quality^{1–4}. However, the incidence of denture fracture has been reported to be as high as 25%, primarily due to mechanical failure⁵. Conventional denture fabrication requires multiple patient visits and involves complex laboratory procedures, increasing costs and introducing additional drawbacks⁶. However, not all denture fractures require complete refabrication; when fractures are localized and minor, repair using cold-polymerized DBRs may be a more practical solution.

Heat-polymerized DBRs have traditionally been used for definitive removable dentures because of their high flexural strength, biocompatibility, and color stability^{7–9}. However, their labor-intensive fabrication and potential for polymerization shrinkage present limitations^{7,8}. Cold-polymerized DBRs, commonly used for repairs and relining, offer ease of use and cost-effectiveness but generally exhibit lower mechanical strength and poor color stability^{3,10–13}. The advancement of three-dimensional (3D) printing technology has introduced an alternative to conventional denture fabrication¹⁴. Among various techniques, digital light processing (DLP) and stereolithography (SLA) —which utilize light polymerization by curing resin layer by layer—are most commonly employed in denture fabrication, producing clinically acceptable fits¹⁵. 3D printing also allows for efficient refabrication using saved computer-aided design (CAD) files, eliminating the need for additional impressions^{16,17}. However, challenges such as interlayer bonding defects and poor color stability remain^{18,19}.

In the oral environment, fluctuating temperatures, mechanical loading, and exposure to various foods can affect the longevity of DBRs^{20,21}. Among these factors, thermal changes play a crucial role in altering the mechanical and esthetic properties of DBRs²¹. For instance, repeated exposure to hot and cold foods may induce

¹Department and Research Institute of Dental Biomaterials and Bioengineering, BK21 FOUR Project, Yonsei University College of Dentistry, Seoul, Republic of Korea. ²Department of Prosthodontics, Yonsei University College of Dentistry, Seoul, Republic of Korea. ³Hospital of Stomatology, Guanghua School of Stomatology, Guangdong Provincial Key Laboratory of Stomatology, Sun Yat-sen University, Guangzhou, China. ⁴Department of Prosthodontics, Geriatric Dentistry and Craniomandibular Disorders, Charité – Universitätsmedizin Berlin, Corporate Member of Freie Universität Berlin and Humboldt-Universität zu Berlin, Berlin, Germany. ✉email: kyungabc@yuhs.ac

thermal stress and color changes, warranting preclinical evaluation^{22–24}. Thermocycling is commonly used in research to simulate temperature fluctuations in a moist oral environment, mimicking the aging process of dental materials^{25–27}.

The shear bond strength of 3D-printed DBRs has been reported to be lower than that of conventional DBRs²⁸, and it significantly decreases after thermocycling²⁹. In contrast, studies have reported conflicting findings regarding the flexural strength of 3D-printed versus heat-polymerized DBRs; however, it is commonly observed that the flexural strength of 3D-printed DBRs significantly decreases after thermocycling^{27,30}. These materials also tend to show inferior color stability compared to heat-polymerized DBRs^{31,32}. Although prior studies provide insight into individual material properties, comprehensive comparisons among various DBR types in terms of shear bond strength (related to repair), flexural strength, and color stability—particularly with respect to thermocycling—remain limited.

Therefore, this study aimed to evaluate the mechanical properties (shear bond strength and flexural strength) and color stability of heat-polymerized, cold-polymerized, and 3D-printed DBRs before and after thermocycling. The null hypotheses were that there would be no significant differences in mechanical properties or color stability among the three DBR types, and that thermocycling would not significantly affect the mechanical properties of the tested DBRs.

Materials and methods

Specimen design

This study utilized heat-polymerized (IvoBase Hybrid; Ivoclar Vivadent AG, Schaan, Liechtenstein), cold-polymerized (PRESS LT; Retec, Rosbach, Germany), and 3D-printed (Denture 3D+; NextDent B.V., Soesterberg, the Netherlands) DBRs. The detailed specifications for each DBR type are summarized in Table 1. For the shear bond strength test, disc-shaped specimens (8 × 2 mm) were designed using commercial CAD software (Autodesk Meshmixer, v3.5; Autodesk, San Francisco). Bar-shaped specimens (3.3 × 10 × 64 mm) were prepared for the flexural strength test, and disc-shaped specimens (10 × 2 mm) were used for the color stability test. All designs were saved in standard tessellation language (STL) format.

A total of 180 specimens were fabricated: 72 for the shear bond strength test, 72 for the flexural strength test, and 36 for the color stability test. Sample size calculation was performed using G*Power software (version 3.1.9.7; Heinrich Heine University Düsseldorf, Germany) based on an A priori power analysis. For the shear bond strength and flexural strength tests, an effect size of 0.35, a significance level (α) of 0.05, and a statistical power ($1 - \beta$) of 0.80 indicated a minimum required sample size of 67 (approximately 11.2 specimens per group). Accordingly, a group size of 12 was adopted to ensure adequate power. The same group size ($n = 12$) was applied to the color stability test to maintain consistency across experiments, corresponding to an effect size of 0.55.

Preparation of Heat-Polymerized DBR specimens

Heat-polymerized DBR specimens (Group HEA) were fabricated using wax discs (Dental Wax; Aidite, Qinhuangdao, China), which were milled using a milling machine (DWX-51D; Roland, Shizuoka, Japan). The wax specimens were affixed to a glass plate, over which type III dental stone (Snow Rock Dental Stone; DK Mungyo, Gimhae, Korea) was poured. After setting, the glass plate was removed, and the stone blocks were trimmed to fit the flasks. Plaster (Mono 70; DK Mungyo) was poured into the lower flask, and an injection channel was positioned over the wax specimens. A separating medium (Acro Sep; GC Corp., Tokyo, Japan) was applied to the plaster before assembling the flasks, which were then filled with additional plaster. After the plaster set, the wax was eliminated through a 10-minute boil-out. The flasks were reassembled, and the heat-polymerized DBR (IvoBase Hybrid; Ivoclar Vivadent AG, Schaan, Liechtenstein) was injected using the IvoBase Injector system (IvoBase Injector; Ivoclar Vivadent AG). Polymerization was performed at 120 °C for 35 min, following the manufacturer's instructions. After polymerization, the specimens were deflasked and trimmed with carbide denture burs (H251ACR and H251EQ; Komet, Lemgo, Germany). Final surface finishing was done under running water using a polishing machine (Metaserv 250; Buehler GmbH, Braunschweig, Germany) with 600-grit silicon carbide sandpaper (SiC Sand Paper; R&B, Daejeon, Korea; Fig. 1).

Preparation of Cold-Polymerized DBR specimens

Cold-polymerized DBR specimens (Group COL) were fabricated using a negative mold technique. First, specimens were 3D-printed using a 3D-printable DBR (Denture 3D+; NextDent B.V.) and a digital light processing (DLP) 3D printer (NextDent5100; NextDent B.V.). These printed specimens were embedded in a hard silicone putty mold (DuoSil Putty Hard; Bukwang, Busan, Korea). After the putty hardened, the printed specimens were removed, forming a negative mold. Cold-polymerized DBR (PRESS LT; Retec) was mixed at a powder-to-liquid ratio of 10 g to 7 g, providing a working time of approximately 5 min. The resin mixture

Group	Material	Composition
HEA	IvoBase Hybrid (Ivoclar Vivadent AG; Schaan, Liechtenstein)	Polymethyl methacrylate 95.5%, plasticizer 3.8%, initiator 0.6%, pigments 0.1%; Methyl methacrylate 95.9%, dimethacrylate (linker) 4.0%, catalyst 0.1%
COL	PRESS LT (Retec Kunststofftechnik GmbH; Rosbach, Germany)	Methyl methacrylate, tetramethylene dimethacrylate
TDP	Denture 3D+ (NextDent B.V.; Soesterberg, The Netherlands)	Ethoxylated bisphenol A dimethacrylate, 7,7,9(or 7,9,9)-trimethyl-4,13-dioxo-3,14-dioxa-12-diazahexadecane-1,16-diy bismethacrylate, 2-hydroxyethyl methacrylate, silicon dioxide, diphenyl (2,4,6-trimethylbenzoyl), phosphine oxide, titanium dioxide

Table 1. Details of denture base resins used in the study.

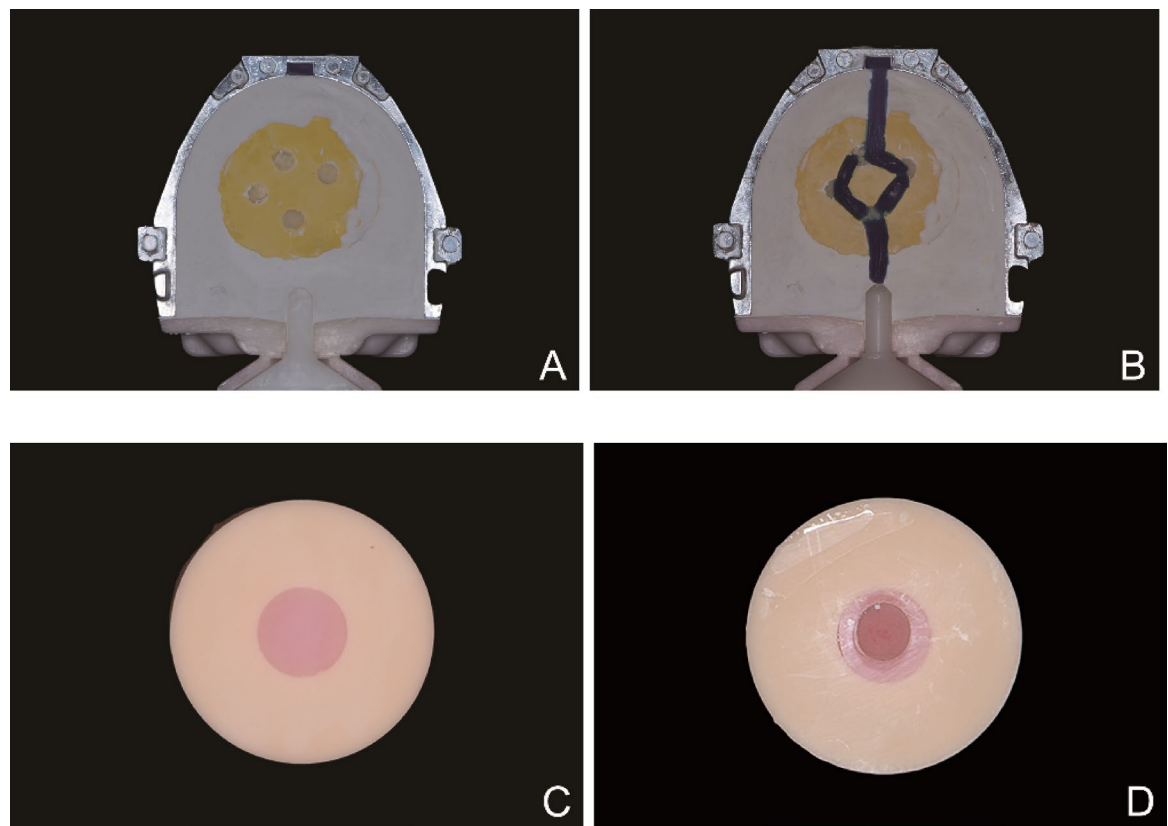


Fig. 1. Sample preparation procedures for group HEA for shear bond strength test. (A) Milled wax specimens embedded in the upper half of the flask. (B) Wax sprues attached. (C) Specimen secured in a stabilization jig. (D) Cold-polymerized denture base resin attached to the specimen. HEA, heat-polymerized denture base resin.

was poured into the mold cavity and polymerized under 2 bar pressure in water at 45 °C for 20 min. After polymerization, the specimens were removed from the mold and prepared for testing.

Preparation of 3D-Printed DBR specimens

3D-printed DBR specimens (Group TDP) were fabricated using the 3D-printable DBR (Denture 3D+; NextDent B.V.) and the 3D-printer (NextDent 5100; NextDent B.V.) Printing was performed horizontally (0° build angle) with a 100 µm layer thickness. After printing, specimens were washed in 94% ethanol for 5 min to remove uncured resin, then post-cured in a polymerization unit (LC-3D Print Box; NextDent B.V.) at 60 °C for 30 min using 405 nm light at ~ 350 mW/cm², as per manufacturer guidelines.

Shear bond strength test

DBR specimens were embedded in cylindrical jigs (25 mm diameter, 13 mm height) fabricated using 3D-printable resin (NextDent Model 2.0; NextDent B.V.). A cold-polymerized DBR (PRESS LT; Retec) was used as the embedding medium. Exposed DBR surfaces were polished with 600-grit silicon carbide sandpaper (SiC Sand Paper; R&B) and sandblasted with 110 µm Al₂O₃ at 4 bar from approximately 10 mm distance for 10 s, standardized across all groups. A water-soluble capsule was placed on the exposed DBR surface, and the cold-polymerized DBR (PRESS LT; Retec) was applied into the capsule. After polymerization, the capsule was rinsed away, leaving an adhered cold-polymerized DBR layer.

Half of the specimens ($n = 12$ per group) were stored in 37 °C distilled water bath for 24 h. The other half underwent 10,000 thermocycles (5–55 °C; 30-second dwell time; 5-second transfer; RB 508, R&B) in distilled water^{30,33}. Shear bond strength was measured using a universal testing machine (Model 3366, Instron Corp., MA) at 0.5 mm/min crosshead speed. Shear bond strength (S) was calculated as:

$$S = \frac{F}{A}$$

where S is shear bond strength (MPa), F is the fracture force (N), and A is the bonded area (mm²) (Fig. 2)^{28,29}.

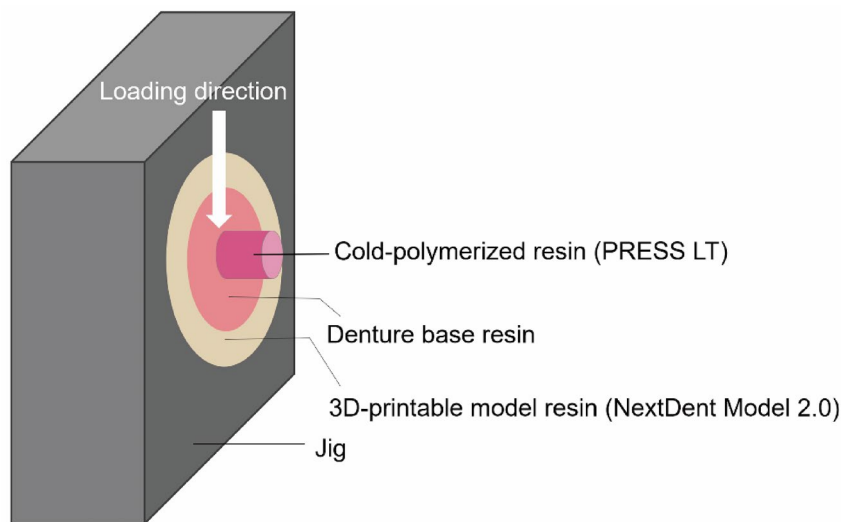


Fig. 2. Schematic diagram of the experimental setup for the shear bond strength test. The load was applied directly to the interface.

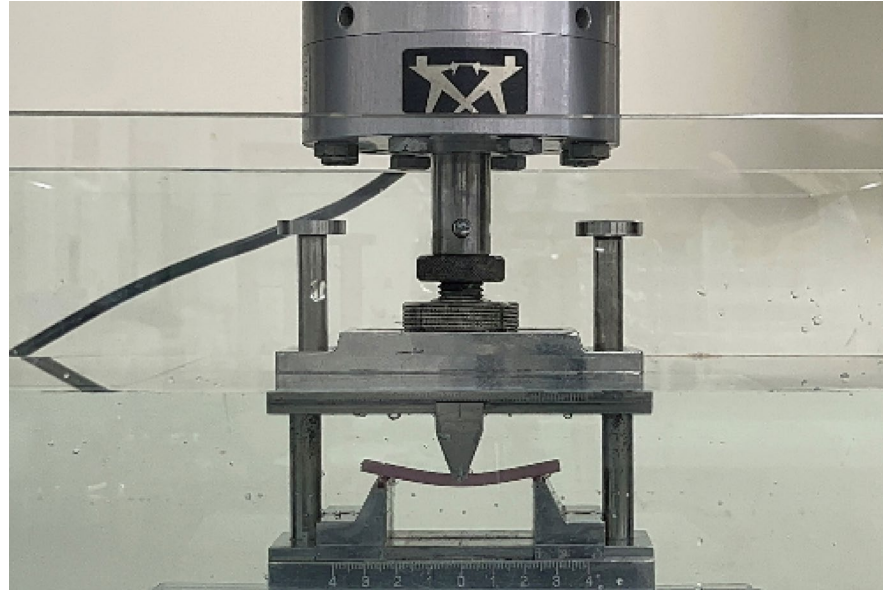


Fig. 3. Flexural strength test of a denture base resin using a universal testing machine (Model 3366, Instron Corp.) in accordance with the International Organization for Standardization 20795-1.

Flexural strength test

A three-point flexural strength test was performed. Half of the bar-shaped specimens ($n=12$ per group) were conditioned in 37 °C distilled water, while the rest underwent 10,000 thermocycles as described above. The support span was 50 mm. Testing was done using a universal testing machine at 5 mm/min crosshead speed (Fig. 3). Flexural strength (σ) was calculated as:

$$\sigma = \frac{3Fl}{2bh^2}$$

where σ is flexural strength (MPa), F is the maximum load (N), l is the distance between the supports (mm), b is specimen width (mm), and h is specimen height (mm)³⁴.

Color stability test

A total of 36 specimens ($n = 12$ per group) were used for the color stability test. Specimens were stored in 37 °C distilled water for 24 h before measurement. Initial L' , a' , and b' values of each specimen were measured

Group	Before thermocycling	After thermocycling
HEA	14.85 \pm 2.02 ^{AA}	7.17 \pm 2.43 ^{AB}
COL	15.76 \pm 2.94 ^{AA}	11.19 \pm 3.48 ^{Bb}
TDP	9.91 \pm 2.57 ^{Ba}	6.89 \pm 1.89 ^{Ab}

Table 2. Shear bond strength (MPa) values. Uppercase letters indicate statistically significant differences among groups, while lowercase letters denote statistically significant differences related to thermocycling.

Group	Before Thermocycling	After Thermocycling
HEA	68.05 \pm 4.25 ^{AA}	67.57 \pm 7.58 ^{AA}
COL	62.53 \pm 5.10 ^{AA}	60.67 \pm 4.57 ^{Ba}
TDP	87.55 \pm 8.42 ^{Ba}	79.79 \pm 2.97 ^{Cb}

Table 3. Flexural strength (MPa) values. Uppercase letters indicate statistically significant differences among groups, while lowercase letters denote statistically significant differences related to thermocycling.

using a colorimeter (Minolta Chroma Meter CR-321; Minolta Corp., Osaka, Japan) under standardized lighting conditions (CIE standard illuminant D65, \sim 6500 K)³⁵. The device was calibrated before each session using the manufacturer's white tile. Each specimen was measured three times, and the average was recorded. After 10,000 thermocycles (same protocol), post-treatment L' , a' , and b' values were measured under identical conditions. The color difference (ΔE_{00}) was calculated using the CIEDE2000 formula:

$$\Delta E_{00} = \sqrt{\left(\frac{\Delta L'}{K_L S_L}\right)^2 + \left(\frac{\Delta C'}{K_C S_C}\right)^2 + \left(\frac{\Delta H'}{K_H S_H}\right)^2 + R_T \left(\frac{\Delta C'}{K_C S_C}\right) \left(\frac{\Delta H'}{K_H S_H}\right)}$$

where $\Delta L'$, $\Delta C'$, and $\Delta H'$ are lightness, chroma, and hue differences, respectively; K_L , K_C , K_H = 1; S_L , S_C , and S_H are compensation factors; and R_T represents the hue rotation adjustment^{31,32}.

Statistical analysis

Statistical analysis was performed using SPSS version 26.0 (IBM Corp., Armonk, NY). Two-way analysis of variance (ANOVA) with post hoc tests were conducted for the shear bond strength and flexural strength analyses. One-way ANOVA with Bonferroni correction was applied for the color stability analysis. Statistical significance was set at $\alpha=0.05$.

Results

For shear bond strength, significant main effects were found for both group ($F=22.690$, $p<0.001$, $\eta^2=0.022$) and thermocycling ($F=68.416$, $p<0.001$, $\eta^2=0.586$), as well as a significant interaction between group and thermocycling ($F=4.976$, $p=0.010$, $\eta^2=0.304$). All groups showed a significant decrease in shear bond strength following thermocycling ($p<0.001$ for groups HEA and COL; $p=0.006$ for group TDP; Table 2). The percentage reduction in shear bond strength post-thermocycling was 51.75% for group HEA, 29.00% for group COL, and 30.41% for group TDP. Before thermocycling, group TDP exhibited significantly lower shear bond strength than groups HEA and COL ($p<0.001$). However, after thermocycling, group TDP presented values comparable to group HEA ($p>0.999$).

For flexural strength, significant main effects were observed for group ($F=92.138$, $p<0.001$, $\eta^2=0.736$) and thermocycling ($F=6.061$, $p<0.001$, $\eta^2=0.084$), while the interaction between group and thermocycling was not statistically significant ($F=2.664$, $p=0.077$, $\eta^2=0.075$). Thermocycling did not affect the flexural strength of HEA ($p=0.841$) or COL ($p=0.434$). However, it significantly reduced the flexural strength of group TDP ($p=0.002$), although its values remained significantly higher than those of the other two groups, both before and after thermocycling ($p<0.001$ compared with groups HEA and COL; Table 3). The percentage reduction in flexural strength after thermocycling was 0.71% in group HEA, 2.93% in group COL, and 8.87% in group TDP.

For color stability, all pairwise comparisons among the three groups showed significant differences. Group HEA exhibited the highest color stability, followed by group COL, and group TDP showed the lowest (HEA vs. COL, $p=0.007$; HEA vs. TDP, $p<0.001$; COL vs. TDP, $p=0.002$) (Table 4).

Discussion

The null hypotheses were rejected, as the three types of DBRs demonstrated significant differences in mechanical properties and color stability. Additionally, thermocycling significantly affected the shear bond strength of all DBR types and the flexural strength of the 3D-printed specimens. Thermocycling was used to simulate intraoral conditions, where dental materials are subjected to continuous temperature fluctuations. These fluctuations induce thermal stress, which may compromise the mechanical and esthetic stability of denture base materials. Therefore, evaluating material responses to thermocycling is critical to understanding their long-term durability and clinical performance. In this study, specimens underwent 10,000 thermocycles between 5 °C and 55 °C with a 30-second dwell time in distilled water, simulating approximately one year of clinical use²³. This short-

Group	ΔE_{00}
HEA	$0.83 \pm 0.47^{\text{A}}$
COL	$1.94 \pm 1.34^{\text{B}}$
TDP	$3.23 \pm 0.18^{\text{C}}$

Table 4. Color difference (ΔE_{00}) values. Uppercase letters indicate statistically significant differences among groups.

term aging protocol was selected to evaluate the initial stability and repairability of 3D-printed DBRs, which are relatively new. Distilled water was used as the immersion medium to standardize thermal stress and avoid variability from biological fluids. Future studies may incorporate extended thermocycling durations and artificial saliva immersion to better mimic the oral environment.

The bond integrity of DBRs remains a critical factor for clinical longevity, particularly when repairs are required during the lifespan of the prosthesis. The results of the shear bond strength test revealed a significant decline in bond strength after thermocycling across all groups, underscoring the impact of thermal fatigue on adhesion between DBRs and repair materials. These reductions are likely due to repeated expansion and contraction of the polymer matrix, which can lead to microstructural degradation and bond failure³⁶. Notably, after thermocycling, the shear bond strength of 3D-printed DBRs was comparable to that of heat-polymerized DBRs, indicating clinically acceptable repairability. Since post-aging performance is more clinically relevant than pre-aging properties, this finding supports the viability of 3D-printed DBRs for repaired prostheses. Further studies should explore the effects of surface treatments, such as sandblasting, mechanical roughening, or bonding agents, on improving bond strength. Group COL exhibited higher shear bond strength than group TDP both before and after thermocycling, likely due to the chemical similarity between the base and repair materials, as the same cold-polymerized resin was used. This is consistent with a previous finding, which suggests that using chemically compatible materials for repair enhances bond strength and fracture resistance³⁷.

The minimum required flexural strength is 65 MPa for heat-polymerized DBRs and 60 MPa for cold-polymerized DBRs, as specified in the International Organization for Standardization (ISO) 20795-1³⁴. All groups in the present study exceeded these thresholds both before and after thermocycling, demonstrating compliance with international standards. Notably, group TDP consistently showed the highest flexural strength across all conditions, supporting its potential as an alternative to conventional heat-polymerized DBRs. Several factors may account for the superior flexural strength observed in the present study: the horizontal printing orientation, which may have enhanced interlayer cohesion and shifted the layer build-up of the printing direction to be perpendicular to load direction^{38,39}; the extended post-polymerizing protocol (30 min at 60 °C), which may have increased the degree of conversion^{40,41}; and the specific formulation of Denture 3D+ (NextDent), which may have contributed to improved mechanical performance.

Intraoral factors such as saliva, food and beverages, and smoking can influence the color stability of DBRs^{42,43}. In this study, color changes were assessed using the CIEDE2000 (ΔE_{00}) formula, which offers perceptually accurate and clinically meaningful data^{44,45}. For practical evaluation of color differences based on ΔE_{00} , two thresholds are widely used: the perceptibility threshold (PT) and the acceptability (AT) threshold⁴⁶. However, the literature varies regarding the reported numerical values of these thresholds, most of which have been applied to evaluate ceramic materials^{45,47}. In a study determining color difference thresholds for DBRs, the PT and AT were proposed as 1.72 and 4.08, respectively⁴⁸. Based on these thresholds, the color change in Group TDP can be considered perceptible to at least half of the observers. This suggests that current 3D-printed DBRs may have limitations in long-term esthetic stability. Clinicians should exercise caution when selecting these materials for anterior restorations or in cases where esthetic outcomes are critical. Nevertheless, 3D-printed DBRs show promise for posterior or interim prostheses, where esthetic demands are lower. Additive manufacturing may have led to this issue by producing materials with lower degrees of polymerization and higher porosity, leading to increased water sorption and susceptibility to discoloration^{49–52}. Optimizing post-polymerizing protocols and improving resin formulations may enhance their esthetic durability.

This study has several limitations. First, as an *in vitro* investigation, it does not fully replicate the complexity of *in vivo* conditions, such as microbial activity, pH cycling, mechanical brushing, and the presence of saliva, all of which may influence material degradation. Second, only one commercial product per material type was tested, limiting the generalizability of the findings across different formulations. Third, this study did not examine specific bonding protocols for 3D-printed DBRs, which may impact repair outcomes. Additionally, the repaired prostheses may exhibit different structural integrity compared to intact ones, however, the flexural strength of repaired specimens was not tested. Future research should evaluate the mechanical performance of repaired DBRs, for example, by incorporating cold-cured resin into centrally positioned areas within base resin specimens, as suggested in a recent study⁵³. Additional investigations into extended aging protocols, alternative repair materials, and various 3D-printing parameters (e.g., layer thickness, build orientation, post-polymerizing conditions) are warranted to further optimize the clinical performance of 3D-printed DBRs.

Conclusions

Within the limitations of this *in vitro* study, repairing denture bases fabricated with 3D-printed DBRs using cold-polymerized DBRs may offer a viable short-term solution. Additionally, 3D-printed DBRs exhibited superior flexural strength, both initially and after simulated short-term use. However, noticeable color changes

were observed in 3D-printed DBRs following thermocycling, suggesting the need for further improvement in their color stability.

Data availability

Data are available upon reasonable request from the corresponding author.

Received: 7 March 2025; Accepted: 14 October 2025

Published online: 19 November 2025

References

1. Jagger, D., Harrison, A. & Jandt, K. The reinforcement of dentures. *J. Oral Rehabil.* **26**, 185–194 (1999).
2. An, S., Evans, J. L., Hamlet, S. & Love, R. M. Incorporation of antimicrobial agents in denture base resin: A systematic review. *J. Prosthet. Dent.* **126**, 188–195 (2021).
3. Polyzois, G. L., Tarantili, P. A., Frangou, M. J. & Andreopoulos, A. G. Fracture force, Deflection at fracture, and toughness of repaired denture resin subjected to microwave polymerization or reinforced with wire or glass fiber. *J. Prosthet. Dent.* **86**, 613–619 (2001).
4. Gad, M. M. et al. Repair strength of 3D-printed denture base resins: Effect of surface treatment and repair material type. *J. Prosthodont.* n/a.
5. de Paula, M. S. et al. A prospective cohort on the incidence of fractures in single-implant mandibular overdentures. *J. Dent.* **103**, 103521 (2020).
6. Clark, W. A., Brazile, B., Matthews, D., Solares, J. & De Kok, I. J. A comparison of conventionally versus digitally fabricated denture outcomes in a university dental clinic. *J. Prosthodont.* **30**, 47–50 (2021).
7. Öztürk, Z. & Tosun, B. Comparison of 3D printed and conventional denture base materials in terms of durability and performance characteristics. *Sci. Rep.* **15**, 18234 (2025).
8. Faot, F., da Silva, W. J., da Rosa, R. S., Bel Cury, D., Garcia, R. C. & A. A. & Strength of denture base resins repaired with auto- and visible light-polymerized materials. *J. Prosthodont.* **18**, 496–502 (2009).
9. Alqahtani, A. Y. et al. Polymeric Denture Base Materials: A Review. *Polymers (Basel)* **15**, 3258 (2023).
10. Stanford, J. W., Burns, C. L. & Paffenbarger, G. C. Self-curing resins for repairing dentures: some physical properties. *J. Am. Dent. Association.* **51**, 307–315 (1955).
11. Rached, R. & Powers, J. Del Bel Cury, A. Efficacy of conventional and experimental techniques for denture repair. *J. Oral Rehabil.* **31**, 1130–1138 (2004).
12. AlQahtani, M. & Haralur, S. B. Influence of different repair acrylic resin and thermocycling on the flexural strength of denture base resin. *Medicina* **56**, 50 (2020).
13. Bohra, P. K., Ganesh, P. R., Reddy, M. M., Ebenezar, A. V. & Sivakumar, G. Colour stability of heat and cold cure acrylic resins. *J. Clin. Diagn. Res.* **9**, Zc12–15 (2015).
14. Anadioti, E., Musharbash, L., Blatz, M. B., Papavasiliou, G. & Kambosiora P. 3D printed complete removable dental prostheses: a narrative review. *BMC Oral Health.* **20**, 343 (2020).
15. Tosun, O. N., Bilmenoglu, C. & Özdemir, A. K. Comparison of denture base adaptation between additive and conventional fabrication techniques. *J. Prosthodont.* **32**, e64–e70 (2023).
16. Goodacre, B. J. & Goodacre, C. J. Additive manufacturing for complete denture fabrication: A narrative review. *J. Prosthodont.* **31**, 47–51 (2022).
17. Takeda, Y., Lau, J., Nouh, H. & Hirayama, H. A 3D printing replication technique for fabricating digital dentures. *J. Prosthet. Dent.* **124**, 251–256 (2020).
18. Alharbi, N., Osman, R. & Wismeijer, D. Effects of build direction on the mechanical properties of 3D-printed complete coverage interim dental restorations. *J. Prosthet. Dent.* **115**, 760–767 (2016).
19. Gad, M. M. et al. Effect of daily immersion of different beverages on the surface roughness and color stability of 3D-printed denture base resins. *J. Prosthodont.* <https://doi.org/10.1111/jopr.13993> (2024).
20. Michailescu, P., Marciano, J., Grieve, A. & Abadie, M. An in vivo recording of variations in oral temperature during meals: a pilot study. *J. Prosthet. Dent.* **73**, 214–218 (1995).
21. Barclay, C., Spence, D. & Laird, W. Intra-oral temperatures during function. *J. Oral Rehabil.* **32**, 886–894 (2005).
22. Goiato, M. C. et al. Effect of thermal cycling and disinfection on colour stability of denture base acrylic resin. *Gerodontontology* **30**, 276–282 (2013).
23. Gale, M. & Darvell, B. Thermal cycling procedures for laboratory testing of dental restorations. *J. Dent.* **27**, 89–99 (1999).
24. Sulaiman, T. A., Rodgers, B., Suliman, A. A. & Johnston, W. M. Color and translucency stability of contemporary resin-based restorative materials. *J. Esthet. Restor. Dent.* **33**, 899–905 (2021).
25. Choi, J. E. et al. Adhesive evaluation of three types of resilient denture liners bonded to heat-polymerized, autopolymerized, or CAD-CAM acrylic resin denture bases. *J. Prosthet. Dent.* **120**, 699–705 (2018).
26. Zeidan, A. A. E. et al. Evaluation of the effect of different construction techniques of CAD-CAM Milled, 3D-Printed, and polyamide denture base resins on flexural strength: an in vitro comparative study. *J. Prosthodont.* **32**, 77–82 (2023).
27. Temizci, T. & Bozoğulları, H. N. Effect of thermal cycling on the flexural strength of 3-D printed, CAD/CAM milled and heat-polymerized denture base materials. *BMC Oral Health.* **24**, 357 (2024).
28. Gibreel, M. et al. Effect of different surface treatments on shear bond strength of autopolymerizing repair resin to denture base materials processed with different technologies. *J. Prosthodont. Res.* **68**, 549–557 (2024).
29. Li, P., Krämer-Fernandez, P., Klink, A., Xu, Y. & Spintzyk, S. Repairability of a 3D printed denture base polymer: effects of surface treatment and artificial aging on the shear bond strength. *J. Mech. Behav. Biomed. Mater.* **114**, 104227 (2021).
30. Gad, M. M. et al. Strength and surface properties of a 3D-printed denture base polymer. *J. Prosthodont.* **31**, 412–418 (2022).
31. Falahchai, M., Ghavami-Lahiji, M., Rasaie, V., Amin, M. & Neshandar Asli, H. Comparison of mechanical properties, surface roughness, and color stability of 3D-printed and conventional heat-polymerizing denture base materials. *J. Prosthet. Dent.* **130**, 266e261–266e268 (2023).
32. Gad, M. A., Abdelhamid, A. M., ElSamahy, M., Abolghait, S. & Hanno, K. I. Effect of aging on dimensional accuracy and color stability of CAD-CAM milled and 3D-printed denture base resins: a comparative in-vitro study. *BMC Oral Health.* **24**, 1124 (2024).
33. Kim, G. Y., Moon, H. S., Kwon, J. S. & Oh, K. C. An in vitro evaluation of bond strength and failure behavior between 3D-printed cobalt-chromium alloy and different types of denture base resins. *J. Dent.* **147**, 105119 (2024).
34. ISO 20795-1. Dentistry. *Base polymers. Part 1: Denture base polymers* (International Organization for Standardization, 2013).
35. Lee, Y. K., Yu, B., Lim, J. I. & Lim, H. N. Perceived color shift of a shade guide according to the change of illuminant. *J. Prosthet. Dent.* **105**, 91–99 (2011).
36. Marra, J., De Souza, R. F., Barbosa, D. B., Pero, A. C. & Compagnoni, M. A. Evaluation of the bond strength of denture base resins to acrylic resin teeth: effect of thermocycling. *J. Prosthodontics: Implant Esthetic Reconstr. Dentistry.* **18**, 438–443 (2009).

37. Faot, F., Da Silva, W. J., Rosa, D., Bel Cury, R. S. D., Garcia, R. C. & A. A. & M. R. Strength of denture base resins repaired with auto-and-visible light-polymerized materials. *J. Prosthodontics: Implant Esthetic Reconstr. Dentistry*. **18**, 496–502 (2009).
38. Al-Dulaijan, Y. A. et al. Effect of printing orientation and postcuring time on the flexural strength of 3D-Printed resins. *J. Prosthodont.* **32**, 45–52 (2023).
39. Keßler, A., Hickel, R. & Ilie, N. *<1> In vitro investigation of the influence of printing direction on the flexural strength, flexural modulus and fractographic analysis of 3D-printed temporary materials</i>*. *Dent. Mater. J.* **40**, 641–649 (2021).
40. Li, P., Lambart, A. L., Stawarczyk, B., Reymus, M. & Spintzyk, S. Postpolymerization of a 3D-printed denture base polymer: impact of post-curing methods on surface characteristics, flexural strength, and cytotoxicity. *J. Dent.* **115**, 103856 (2021).
41. AlRumaih, H. S. & Gad, M. M. The effect of 3D printing layer thickness and Post-Polymerization time on the flexural strength and hardness of denture base resins. *Prosthesis* **6**, 970–978 (2024).
42. Bonatti, M. R. et al. The effect of polymerization cycles on color stability of microwave-processed denture base resin. *J. Prosthodontics: Implant Esthetic Reconstr. Dentistry*. **18**, 432–437 (2009).
43. Arocha, M. A. et al. Colour stainability of indirect CAD-CAM processed composites vs. conventionally laboratory processed composites after immersion in staining solutions. *J. Dent.* **42**, 831–838 (2014).
44. Gómez-Polo, C. et al. Comparison of the CIELab and CIEDE2000 color difference formulas. *J. Prosthet. Dent.* **115**, 65–70 (2016).
45. Ghinea, R. et al. Color difference thresholds in dental ceramics. *J. Dent.* **38**, e57–e64 (2010).
46. ISO/TR 28642. *Dentistry: Guidance on colour measurement* (International Organization for Standardization, 2016).
47. Paravina, R. D. et al. Color difference thresholds in dentistry. *J. Esthet Restor. Dent.* **27**, S1–S9 (2015).
48. Ren, J., Lin, H., Huang, Q. & Zheng, G. Determining color difference thresholds in denture base acrylic resin. *J. Prosthet. Dent.* **114**, 702–708 (2015).
49. Kim, M. C., Byeon, D. J., Jeong, E. J., Go, H. B. & Yang, S. Y. Color stability, surface, and physicochemical properties of three-dimensional printed denture base resin reinforced with different nanofillers. *Sci. Rep.* **14**, 1842 (2024).
50. Gad, M. M. et al. Water Sorption, Solubility, and Translucency of 3D-Printed Denture Base Resins. *Dent. J. (Basel)* **10**, 42 (2022).
51. Greil, V., Mayinger, F., Reymus, M. & Stawarczyk, B. Water sorption, water solubility, degree of conversion, elastic indentation modulus, edge chipping resistance and flexural strength of 3D-printed denture base resins. *J. Mech. Behav. Biomed. Mater.* **137**, 105565 (2023).
52. Alfouzan, A. F. et al. Color stability of 3D-printed denture resins: effect of aging, mechanical brushing and immersion in staining medium. *J. Adv. Prosthodont.* **13**, 160–171 (2021).
53. Özatik, S. & Bural Alan, C. Flexural strength of repaired denture base materials manufactured for the CAD-CAM technique. *J. Oral Sci.* **66**, 120–124 (2024).

Author contributions

H.E.C. wrote the main manuscript text and conducted methodology, formal analysis, investigation, and data curation. S.K. performed formal analysis and data curation. G.Y.K. contributed to data curation, visualization, and formal analysis. J.L. conducted methodology, investigation, and data curation. S.P. performed writing—review and editing, formal analysis, and visualization. K.C.O. was responsible for conceptualization, writing—review and editing, resources, supervision, project administration, and funding acquisition. All authors reviewed the manuscript.

Funding

This research was supported by the Basic Science Research Program through the National Research Foundation of Korea (NRF) funded by the Ministry of Education [grant number 2021R1I1A1A01048233].

Declarations

Competing interests

The authors declare no competing interests.

Additional information

Correspondence and requests for materials should be addressed to K.C.O.

Reprints and permissions information is available at www.nature.com/reprints.

Publisher's note Springer Nature remains neutral with regard to jurisdictional claims in published maps and institutional affiliations.

Open Access This article is licensed under a Creative Commons Attribution-NonCommercial-NoDerivatives 4.0 International License, which permits any non-commercial use, sharing, distribution and reproduction in any medium or format, as long as you give appropriate credit to the original author(s) and the source, provide a link to the Creative Commons licence, and indicate if you modified the licensed material. You do not have permission under this licence to share adapted material derived from this article or parts of it. The images or other third party material in this article are included in the article's Creative Commons licence, unless indicated otherwise in a credit line to the material. If material is not included in the article's Creative Commons licence and your intended use is not permitted by statutory regulation or exceeds the permitted use, you will need to obtain permission directly from the copyright holder. To view a copy of this licence, visit <http://creativecommons.org/licenses/by-nc-nd/4.0/>.

© The Author(s) 2025